

# Lower-Hybrid-Drift Wave Turbulence in the Distant Magnetotail

J. D. HUBA

*Science Applications, Inc., McLean, Virginia 22101*

N. T. GLADD AND K. PAPADOPOULOS

*Naval Research Laboratory, Washington, D. C. 20375*

Recent satellite observations of electrostatic and magnetic noise in the distant magnetotail (Gurnett et al., 1976) can be explained by the excitation of the lower-hybrid-drift instability. In particular, it is shown that (1) existence conditions for the lower-hybrid-drift instability can be met, (2) the observed frequency spectra and polarization are in good agreement with the predictions of linear theory, and (3) the observed amplitudes of fluctuations are consistent with the nonlinear theory of this mode. Moreover, the observation of this instability suggests that the anomalous transport properties associated with these waves, which are important in many laboratory devices, may play a crucial role in the macroscopic evolution of magnetotail processes such as field line merging, tearing instabilities, or 'fireballs.'

## 1. INTRODUCTION

An important aspect of magnetospheric physics is understanding the abundant processes associated with microscopic plasma turbulence. Some of these turbulent microscopic processes result in anomalous plasma transport properties (i.e., processes not explainable in terms of classical Coulomb collisions) and hence greatly influence the macroscopic behavior of the magnetospheric plasma. Many of the most dramatic phenomena in the magnetosphere (e.g., magnetic field line reconnection, magnetic substorms, and aurorae) involve turbulent microscopic plasma phenomena in an integral fashion.

We recently proposed [Huba et al., 1977] that the lower-hybrid-drift instability [Krall and Liewer, 1971], an instability of considerable importance in several magnetic fusion confinement systems [e.g., Davidson et al., 1976; Comisso and Griem, 1976], would be operative over large regions of the magnetotail, and, furthermore, may play a significant role in the development of field line reconnection as a source of anomalous resistivity. In this paper we demonstrate that recent experimental measurements of magnetotail turbulence support our theoretical prediction that the lower-hybrid-drift instability is active in the magnetotail. However, the one-dimensional laminar equilibrium used by Huba et al. [1977] is overly simplistic in modeling the plasma sheet, since experimental observations indicate that it is generally a turbulent medium [Frank et al., 1976; Coroniti et al., 1977]. Rather, localized spatial gradients within a much broader plasma sheet are considered to excite lower-hybrid-drift turbulence in the magnetotail.

Gurnett et al. [1976] have made detailed satellite observations of plasma turbulence in the distant magnetotail (23–46  $R_E$ ) and have found broadband electrostatic noise, magnetic noise, and electrostatic electron cyclotron noise. The broadband electrostatic turbulence is the most intense and frequently occurring type and is strongest in the frequency range  $\Omega_i \ll \omega \lesssim \Omega_e$ . The turbulence is observed in regions of strong plasma and magnetic field gradients in the plasma sheet, where reconnection and/or tearing modes are believed to exist. The magnetic noise is observed in the same spatial regions and the same frequency range as the electrostatic noise but occurs less frequently. The electrostatic electron cyclotron turbulence is

only observed occasionally, tending to occur in very hot regions near the neutral line. Gurnett et al. [1976] suggested that the broadband electrostatic noise could be produced by field-aligned currents and that the magnetic noise could be generated by a whistler instability. The electron cyclotron emissions seem to be of the type studied by Fredericks [1971], Young et al. [1973], Ashour-Abdalla and Kennel [1976], and others and will not be discussed in this paper.

In this paper we examine the experimental observations of Gurnett et al. [1976] in the light of theoretical studies of the lower-hybrid-drift instability and find strong evidence for the existence of this instability in terms of existence criteria, spectral characteristics, and amplitude of fluctuations. Furthermore, our theoretical model explains both the broadband electrostatic noise and the magnetic noise within the context of the lower-hybrid-drift instability.

The lower-hybrid-drift instability [Krall and Liewer, 1971; Davidson and Gladd, 1975; Gladd, 1976; Huba and Wu, 1976; Davidson et al., 1977] is a cross-field current driven instability which has been found to be an important anomalous transport mechanism in laboratory plasmas [Davidson et al., 1976; Comisso and Griem, 1976]. The free energy which supports the instability is provided by the cross-field current and inhomogeneities in the plasma and the magnetic field. The scale lengths of the inhomogeneities needed to excite the instability can be many mean ion Larmor radii,  $L_n \lesssim (m_i/m_e)^{1/4} r_{Li}$ , where  $L_n$  is the characteristic scale length of the density inhomogeneity and  $r_{Li}$  is the mean ion Larmor radius. For weaker gradients,  $(m_i/m_e)^{1/2} < L_n/r_{Li} < (m_i/m_e)^{1/4}$ , the lower-hybrid-drift instability transforms into the drift cyclotron instability [Mikhailovskii and Timofeev, 1963; Friedberg and Gerwin, 1977]. The nature of the lower-hybrid-drift instability is twofold. In the presence of strong plasma gradients ( $L_n/r_{Li} \lesssim 1$ ) it is a fluid instability excited through a coupling of a lower-hybrid wave and a drift wave. When plasma inhomogeneities are weak  $(m_e/m_i)^{1/4} > L_n/r_{Li} \gtrsim 1$ , it is a kinetic instability driven by a resonance between ions and a drift wave. An important advantage of this instability over other cross-field current driven instabilities (e.g., ion acoustic instability and Buneman instability) is that it can readily be excited for much weaker drift currents and persists in the regime  $T_e < T_i$ , which is generally believed to be the case in the magnetotail. Moreover, in finite  $\beta$  plasmas both electrostatic turbulence and electromagnetic turbulence are produced by this instability.

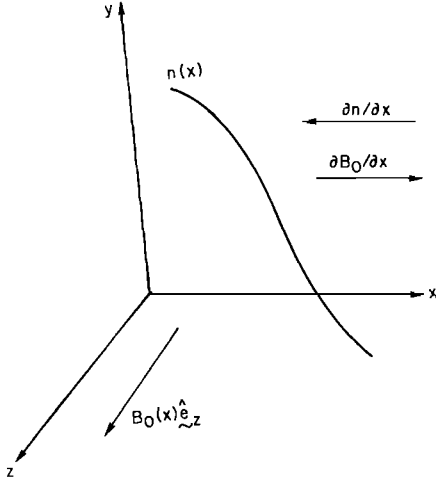


Fig. 1. Slab geometry and background plasma configuration.

We take this opportunity to comment on the fact that although this instability is thought to be important in a number of magnetic fusion confinement systems (e.g., theta pinches, reversed field pinches, and mirror machines), it is very difficult to make detailed laboratory measurements of plasma turbulence of the type made by Gurnett *et al.* [1976] in the magnetotail. Therefore it is interesting to note that the detailed experimental information necessary to decide which of several possible nonlinear mechanisms is most important in saturating the instability and hence in determining the plasma parametric dependence of the various anomalous transport processes may well come from measurements of space plasmas.

The scheme of the paper is as follows. In the next section we present the linear and nonlinear theories of the lower-hybrid-drift instability with an emphasis on the fundamental physical processes. In section 3 we outline the essential features of the observational results. In section 4 we present a detailed comparison of the theoretical predictions with the observational results. In the final section we discuss possible consequences of the observed turbulence in regard to field line reconnection and tearing instabilities in the magnetotail.

## 2. THEORY

### Assumptions and Plasma Configuration

The plasma configuration and slab geometry used in the analysis are shown in Figure 1. The equilibrium magnetic field is  $\mathbf{B} = B(x)\hat{e}_z$ . We assume that the density and the magnetic field vary only in the  $x$  direction and, for simplicity, that the temperature is constant. The electrons drift in the  $y$  direction with a mean fluid velocity ( $m_e \rightarrow 0$ )  $V_{ey} = V_{ae}$ , where  $V_{ae} = -(v_e^2/2\Omega_e) \partial \ln n / \partial x$  is the electron diamagnetic drift velocity and  $n = n_e \approx n_i$  is the density;  $v_\alpha = (2T_\alpha/m_\alpha)^{1/2}$  is the thermal velocity,  $\Omega_\alpha = |e_\alpha|B/m_\alpha c$  is the cyclotron frequency,  $e_\alpha$  is the charge,  $T_\alpha$  is the temperature, and  $m_\alpha$  is the mass, all of species  $\alpha$ . Equilibrium force balance on an ion fluid element in the  $x$  direction requires  $V_{iy} = V_{di}$ , where  $V_{di} = (v_i^2/2\Omega_i) \partial \ln n / \partial x$  is the ion diamagnetic drift velocity. Moreover, we can relate the ion diamagnetic drift velocity to the scale length of the density gradient through  $V_{di}/v_i = \frac{1}{2}r_{Li}/L_n$ , where  $L_n^{-1} = \partial \ln n / \partial x$ . The electrons are assumed to be magnetized, while the ions are treated as unmagnetized. This is a reasonable assumption, since we are considering waves such that  $\Omega_i \ll \omega \ll \Omega_e$  and  $kr_{Li} \gg 1$ , where  $r_{L\alpha} = v_\alpha/\Omega_\alpha$  is the mean Larmor radius of species  $\alpha$ . We consider only flute perturbations ( $\mathbf{k} \cdot \mathbf{B} = 0$ ) and

assume  $k_y^2 \gg k_x^2 \gg (\partial \ln n / \partial x)^2$ ,  $(\partial \ln B / \partial x)^2$ , which justifies the use of the local approximation [Krall, 1968]. Finally, we assume that the plasma is weakly inhomogeneous in the sense that  $r_{Le}^2(\partial \ln n / \partial x)^2 \ll 1$  and  $r_{Le}^2(\partial \ln B / \partial x)^2 \ll 1$ .

### Linear Theory

A comprehensive discussion of the linear theory of the lower-hybrid-drift instability has been given by Davidson *et al.* [1977]. We only present the basic results of the theory at this time and refer the reader to Davidson *et al.* [1977] for details.

The local equilibrium distribution functions of the electrons and ions are

$$F_{e0} = \frac{n(x)}{(\pi v_e^2)^{3/2}} \left[ 1 - \frac{v_y}{\Omega_e L_n} \right] \exp[-v^2/v_e^2]$$

and

$$F_{i0} = \frac{n(x)}{(\pi v_i^2)^{3/2}} \exp[-(v_x^2 + (v_y - V_{di})^2 + v_z^2)/v_i^2]$$

respectively, where  $V_{di} = (v_i^2/2\Omega_i)[\partial \ln n / \partial x]_{x=x_0}$  and the perturbations are assumed to be well localized about  $x = x_0$ . We emphasize that  $F_{i0}$  is a valid local equilibrium even when the ion orbits are large (i.e.,  $r_{Li}/L_n \approx 1$ ) [Davidson and Gladd, 1977]. Following Davidson *et al.* [1977] the equations which describe the lower-hybrid-drift instability are

$$D_{xx}(\omega, k)\delta\hat{E}_x + D_{xy}(\omega, k)\delta\hat{E}_y = 0 \quad (1)$$

$$D_{yx}(\omega, k)\delta\hat{E}_x + D_{yy}(\omega, k)\delta\hat{E}_y = 0 \quad (2)$$

where  $\delta\mathbf{E} = \delta\hat{\mathbf{E}} \exp[i(ky - \omega t)]$ ,

$$D_{xx}(\omega, k) = 1 - \frac{c^2 k^2}{\omega^2} - \frac{2\omega_{pe}^2}{\omega^2} \Phi_1 \quad (3)$$

$$D_{xy}(\omega, k) = -D_{yx}(\omega, k) = 2i \frac{\omega_{pe}}{\omega} \frac{\omega_{pe}}{kv_e} \Phi_2 \quad (4)$$

$$D_{yy}(\omega, k) = 1 + \frac{2\omega_{pi}^2}{k^2 v_i^2} [1 + \xi_i Z(\xi_i)] + \frac{2\omega_{pe}^2}{k^2 v_e^2} (1 - \Phi_3) \quad (5)$$

where  $\xi_i = (\omega - kV_{di})/kv_i$ ,  $Z(\xi) = (\pi)^{-1/2} \int_{-\infty}^{\infty} dx \exp(-x^2)/(x - \xi)$ , and  $\Phi_1$ ,  $\Phi_2$ , and  $\Phi_3$  are defined by

$$\Phi_j = \Lambda \int_0^\infty ds^2 \frac{F_j \exp(-s^2)}{\omega - k\tilde{V}_B s^2} \quad j = 1, 2, 3 \quad (6)$$

where  $F_1 = [sJ_1(\mu)]^2$ ,  $F_2 = sJ_0(\mu)J_1(\mu)$ ,  $F_3 = J_0^2(\mu)$ ,  $\mu = kr_{Le}s$ ,  $s = v_\perp/v_e$ ,  $\Lambda = \omega - kV_{ae}$ ,  $\tilde{V}_B = -(v_e^2/2\Omega_e) \partial \ln B / \partial x$ , and  $J_n(\mu)$  is the Bessel function of order  $n$ . The fluctuating magnetic field associated with the electromagnetic oscillations is given by

$$\delta\hat{\mathbf{B}}_z = -(ck/\omega)\delta\hat{E}_x \quad (7)$$

The dispersion equation can be found from  $\det[\mathbf{D}] = D_{xx}D_{yy} - D_{xy}D_{yx} = 0$ , which yields

$$D(\omega, k) = \left[ 1 + \frac{2\omega_{pi}^2}{k^2 v_i^2} [1 + \xi_i Z(\xi_i)] + \frac{2\omega_{pe}^2}{k^2 v_e^2} (1 - \Phi_3) \right] + \frac{2\omega_{pe}^2}{c^2 k^2} \frac{2\omega_{pe}^2}{k^2 v_e^2} \Phi_2^2 \left( 1 + \frac{2\omega_{pe}^2}{c^2 k^2} \Phi_1 \right)^{-1} = 0 \quad (8)$$

where we have assumed  $\omega^2 \ll c^2 k^2$ . We emphasize that (8) is valid for plasmas of arbitrary  $\beta$  ( $= 8\pi n(T_e + T_i)/B^2$ ), an important consideration in modeling the magnetotail. The first term in (8) represents the electrostatic contribution to the mode, while the second term contains the electromagnetic

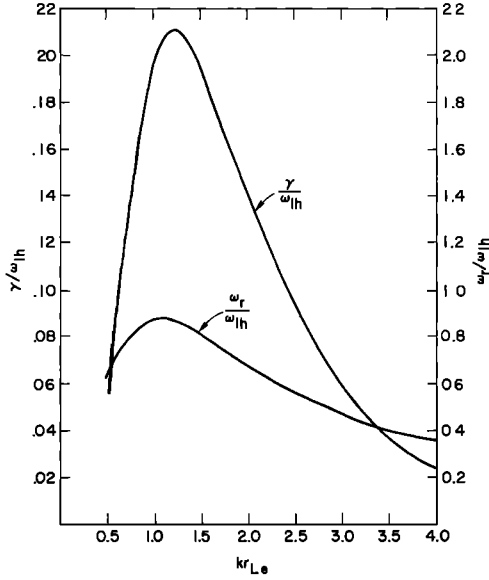


Fig. 2. Spectrum of unstable lower-hybrid-drift waves for  $V_{dt}/v_i = 1.0$ ,  $T_e/T_i = 0.5$ ,  $m_e/m_i = 1/1836$ ,  $\beta = 1.0$ , and  $\omega_{pe}^2/\Omega_e^2 = 125$ .

corrections. Moreover, the  $\nabla B$  orbit modifications of the electrons are treated properly, since they can give rise to important electron-wave resonances [Huba and Wu, 1976].

A qualitative understanding of the lower-hybrid-drift instability can be obtained if we consider only electrostatic oscillations ( $\omega_{pe}^2 \ll c^2 k^2$ ) and cold electrons ( $T_e \rightarrow 0$ ). In this limit, (8) reduces to

$$D(\omega, k) = 1 + \frac{\omega_{pe}^2}{\Omega_e^2} - \frac{2\omega_{pi}^2}{k^2 v_i^2} \frac{kV_{dt}}{\omega} + \frac{2\omega_{pi}^2}{k^2 v_i^2} [1 + \xi_i Z(\xi_i)] = 0 \quad (9)$$

where we have used  $V_{dt} = -(T_i/T_e)V_{de}$ . Two types of instability can occur, depending on the magnitude of the drift velocity. We now examine each case separately.

$V_{dt} \gg v_i$  (*fluid instability*). Assuming that  $V_{dt} \gg v_i$  and  $\omega \gg kv_i$  allows us to make the approximation  $Z(\xi) \approx -1/\xi - 1/2\xi^3$ . It is easily shown that (9) becomes

$$D(\omega, k) = 1 + \frac{\omega_{pe}^2}{\Omega_e^2} - \frac{\omega_{pi}^2}{(\omega - kV_{dt})^2} - \frac{2\omega_{pi}^2}{k^2 v_i^2} \frac{kV_{dt}}{\omega} = 0 \quad (10)$$

which can be rewritten as

$$1 - \frac{(\omega - kV_{dt})^2}{\omega_{lh}^2} \left( 1 - \frac{kV_{dt}}{\omega} \frac{2\omega_{lh}^2}{k^2 v_i^2} \right) = 0 \quad (11)$$

where  $\omega_{lh} = \omega_{pi}/(1 + \omega_{pe}^2/\Omega_e^2)^{1/2}$  is the generalized lower-hybrid frequency. Analysis of (11) indicates that an instability can occur when  $\omega - kV_{dt} < 0$  with  $\omega_r \approx \gamma \approx \omega_{lh}$  [Krall and Liewer, 1971]. In this situation a Doppler-shifted lower-hybrid wave ( $\omega_1 - kV_{dt} = \pm\omega_{lh}$ ) is coupled to a drift wave ( $\omega_2 = kV_{dt}(2\omega_{lh}^2/k^2 v_i^2)$ ), as shown in (11).

$V_{dt} \ll v_i$  (*kinetic instability*). In this limit we assume  $\omega \ll kv_i$  so that  $Z(\xi) \approx i(\pi^{1/2}k/|k|)$ . We find that (7) becomes

$$D(\omega, k) = 1 + \frac{\omega_{pe}^2}{\Omega_e^2} - \frac{2\omega_{pi}^2}{k^2 v_i^2} \frac{kV_{dt}}{\omega} + \frac{2\omega_{pi}^2}{k^2 v_i^2} \left[ 1 + \frac{\omega - kV_{dt}}{|k|v_i} i(\pi^{1/2}) \right] = 0 \quad (12)$$

It readily follows from (12) that for  $\gamma \ll \omega_r$ ,

$$\omega_r = kV_{dt} \frac{2\omega_{pi}^2}{k^2 v_i^2} \left( 1 + \frac{2\omega_{pi}^2}{k^2 v_i^2} + \frac{\omega_{pe}^2}{\Omega_e^2} \right)^{-1} \quad (13)$$

and

$$\gamma = -(\pi^{1/2}) \frac{\omega_r - kV_{dt}}{kv_i} \frac{\omega_r^2}{kV_{dt}} \quad (14)$$

Clearly, an instability is possible ( $\gamma > 0$ ) when  $\omega_r - kV_{dt} < 0$ . The instability is produced by ions in resonance with the drift wave (equation (13)). Maximizing  $\gamma$  with respect to  $k$ , we may easily show that

$$\gamma_M = [(2\pi)^{1/2}/8](V_{dt}/v_i)^2 \omega_{lh} \quad (15)$$

$$\omega_M = (1/2^{1/2})(V_{dt}/v_i) \omega_{lh} \quad (16)$$

and  $k_M = 2^{1/2} \omega_{lh}/v_i$ , the subscript  $M$  denoting values corresponding to maximum growth. Although it has been assumed that  $V_{dt}^2 \ll v_i^2$ , numerical computations verify that these expressions are in fact accurate up to  $V_{dt} \sim v_i$ .

For parameters typical of the magnetotail the kinetic instability is likely to dominate, since it corresponds to inhomogeneity scale lengths greater than or about the mean ion Larmor radius ( $r_{Li} \partial \ln n / \partial x \lesssim 1$ ). However, in general, the approximations made in deriving (1)-(16) are not valid in the magnetotail, and a numerical solution of (8) is required to determine the frequency and growth rate of the wave.

To illustrate the wave characteristics of (8) for typical magnetotail parameters, we present Figures 2 and 3. Figure 2 is a spectrum of unstable waves for  $V_{dt}/v_i = 1.0$  ( $L_n/r_{Li} = 0.5$ ),  $T_e/T_i = 0.5$ ,  $m_e/m_i = 1/1836$ ,  $\beta = 1.0$ , and  $\omega_{pe}^2/\Omega_e^2 = 125$ . The growth rate has a relatively broad spectrum ( $0.5 < kr_{Le} < 5$ ) and achieves a maximum value of  $\gamma_M \approx 0.21\omega_{lh}$  for  $kr_{Le} \approx 1.2$ . The real frequency exhibits the same qualitative behavior as the growth rate with a maximum value  $\omega_M \approx 0.86\omega_{lh}$ . Figure 3 plots the normalized maximum growth rate (as a function of  $k$ ) versus  $V_{dt}/v_i$  for  $\beta = 0.25, 1.00$ , and  $2.50$  and  $T_e/T_i = 0.5$ ,  $\omega_{pe}^2/\Omega_e^2 = 125$ , and  $m_i/m_e = 1836$ . We note that in the strong drift regime ( $V_{dt} > v_i$ ) the growth rate can attain large values ( $\gamma \sim \omega_{lh}$ ). Moreover, the stabilizing nature of  $\beta$  is clearly

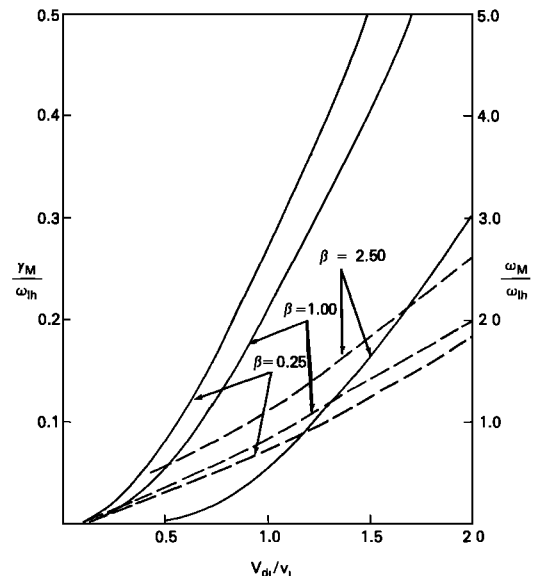


Fig. 3. Maximum growth rate (solid curve) and corresponding real frequency (dashed curve) versus  $V_{dt}/v_i$  for  $\beta = 0.25, 1.00$ , and  $2.50$  and  $T_e/T_i = 0.5$ ,  $m_e/m_i = 1/1836$ , and  $\omega_{pe}^2/\Omega_e^2 = 125$ .

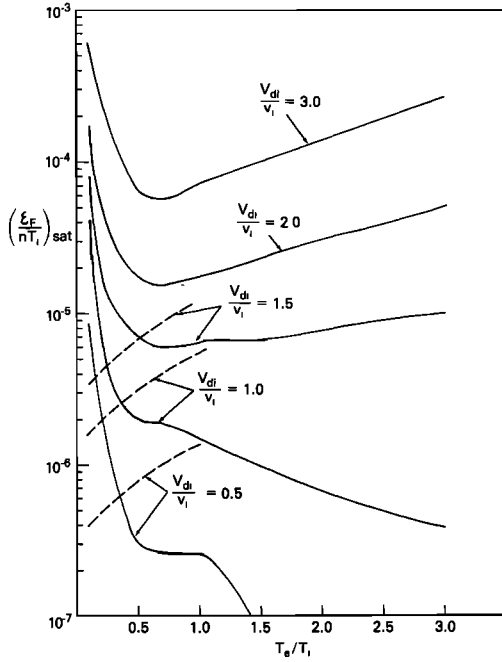


Fig. 4. Saturation energies due to electron resonance broadening (solid curve) and current relaxation (dashed curve) as a function of  $T_e/T_i$  and  $V_{dh}/v_i$  for  $\beta = 1.0$  and  $\omega_{pe}^2/\Omega_e^2 = 100$ .

shown, a point which is relevant to the magnetotail, as will be seen in section 4.

We comment that for  $\mathbf{k} \cdot \mathbf{B} \neq 0$  the growth rate of the mode decreases owing to electron Landau damping. The range of  $k_{\parallel}$  permitted can be determined from  $\omega/k_{\parallel} \gtrsim 2v_e$ , which can be written as

$$\frac{k_{\parallel}}{k_{\perp}} \lesssim \frac{1}{4} \frac{V_{dh}}{v_i} \left( \frac{T_i}{T_e} \right)^{1/2} \left( \frac{m_e}{m_i} \right)^{1/2}$$

where we have assumed  $V_{dh} < v_i$ . Thus the range of unstable waves in  $k_{\parallel}$  space is generally quite small.

We finally note that our model only considers  $\mathbf{B} = B_0 \hat{e}_z$ , which is reasonable, since we are interested in localized spatial structures within the plasma sheet. However, it should be noted that the inclusion of a weak normal component does not alter our results. On the other hand, if the normal component of  $\mathbf{B}$  produces a radius of magnetic curvature comparable to the scale length of the ion pressure gradient, then the mode can be stabilized or destabilized depending on local plasma conditions [Krall and McBride, 1976].

### Nonlinear Theory

Although the linear theory of the lower-hybrid-drift instability is well understood, the nonlinear theory of the instability is not. We briefly discuss each of the nonlinear analyses presented thus far, with an emphasis on obtaining estimates of the saturation amplitude of the unstable waves. This is perhaps the most important aspect of any nonlinear calculation, since the functional form of the anomalous transport coefficients can be obtained from quasi-linear theory, which treats the fluctuation amplitude approximately as a free parameter. Thus a knowledge of the saturation energy (and its parametric dependence) obtained from a nonlinear theory can be used to determine the associated anomalous transport properties of the instability in a straightforward manner based upon quasi-linear theory.

*Quasi-linear theory.* Davidson [1977] has developed a quasi-linear theory of the lower-hybrid-drift instability which is valid for electrostatic perturbations in the low drift velocity ( $V_{dh} < v_i$ ) and cold electron ( $T_e \ll T_i$ ) regime. We comment that these results are insensitive to finite  $\beta$  electromagnetic corrections and can be applied to the magnetotail. He finds that stabilization can occur through either plateau formation in the ion distribution or current relaxation, depending upon the initial conditions of the plasma. These stabilization mechanisms are concerned with the kinetic form of the instability which is driven through an ion-wave resonance (i.e.,  $\gamma \propto \partial F_i / \partial v$ ). It is clear that if  $\partial F_i / \partial v \rightarrow 0$ , then  $\gamma \rightarrow 0$ , which corresponds to the formation of a plateau in the ion distribution. On the other hand, if the free energy available in the system (i.e.,  $W = \frac{1}{2} n m_e V_{dh}^2 [1 + (T_e/T_i)]^2$ , the free energy available from the density inhomogeneity) is expended before  $\partial F_i / \partial v = 0$ , then the instability is stabilized by current relaxation, and the saturation energy can be found by equating the wave energy density to the free energy density. We point out that this stabilization process is not appropriate if the system is being driven by an external force so that  $W \approx \text{const}$ . Following Davidson *et al.* [1977] it can be shown for a hydrogen plasma that (1) if  $|V_{dh}|/v_i > 0.18/(1 + T_e/T_i)$ , then stabilization is due to current relaxation, and the saturation energy is

$$\left( \frac{\epsilon_F}{n T_i} \right)_{\text{sat}}^{cr} = \frac{1}{4} \frac{m_e}{m_i} \frac{V_{dh}^2}{v_i^2} \left( 1 + \frac{T_e}{T_i} \right)^2 \left( 1 + \frac{\omega_{pe}^2}{\Omega_e^2} \right)^{-1} \quad (17)$$

where  $\epsilon_F = |\delta E_y|^2 / 8\pi$  is the field energy density of the electrostatic oscillations and the superscript *cr* denotes current relaxation, or (2) if  $|V_{dh}|/v_i < 0.18/(1 + T_e/T_i)$ , then stabilization is due to plateau formation, and the saturation energy is

$$\left( \frac{\epsilon_F}{n T_i} \right)_{\text{sat}}^{pf} = \frac{2}{45(\pi^{1/2})^2} \left[ \frac{|V_{dh}|}{v_i} \left( 1 + \frac{T_e}{T_i} \right) \right]^5 \left( 1 + \frac{\omega_{pe}^2}{\Omega_e^2} \right)^{-1} \quad (18)$$

where *pf* denotes plateau formation.

*Ion trapping.* Computer simulations of the lower-hybrid-drift instability by Winske and Liewer [1977] indicate that ion trapping stabilizes the instability in the strong drift velocity regime ( $V_{dh} \gtrsim 3v_i$ ). The instability is fluidlike in this regime, and it is possible that a quasi-monochromatic wave develops, so that ions can be trapped in its potential well. Winske and Liewer [1977] consider that  $\omega_{pe}^2/\Omega_e^2 \approx 1$ , so that their results are not strictly applicable to the magnetotail plasma. However, one can obtain the following empirical expression for the saturation energy based on their results:

$$\left( \frac{\epsilon_F}{n T_i} \right)_{\text{sat}}^{it} = 1.77 \times 10^{-2} k^2 \lambda_{di}^2 \left( 1 + \frac{2\omega_r^2}{k^2 v_i^2} \right)^2 \quad (19)$$

where  $\lambda_{di} = v_i / 2\omega_{pi}^{1/2}$  is the ion Debye wavelength and the superscript *it* denotes ion trapping. Thus ion trapping is expected to be an important stabilizing mechanism only in regions of very strong gradients (e.g.,  $L_n/r_{Li} \lesssim \frac{1}{2}$ ).

*Electron resonance broadening.* Huba and Papadopoulos [1978] have shown that electron resonance broadening can effectively stabilize the lower-hybrid-drift instability in finite  $\beta$  plasmas. This saturation mechanism can be understood as follows. From (8) it is clear that an electron-wave resonance can occur when

$$\frac{V_r^2}{v_e^2} = \frac{\omega}{k \bar{V}_B} \approx \frac{V_{dh}}{\bar{V}_B} \approx \frac{1}{\beta} \frac{T_i}{T_e} \quad (20)$$

where  $V_r$  is the perpendicular electron resonant velocity. In the limit  $\beta \rightarrow 0$  or  $T_e \rightarrow 0$  it is seen that  $V_r^2 \gg v_e^2$ , and hence few

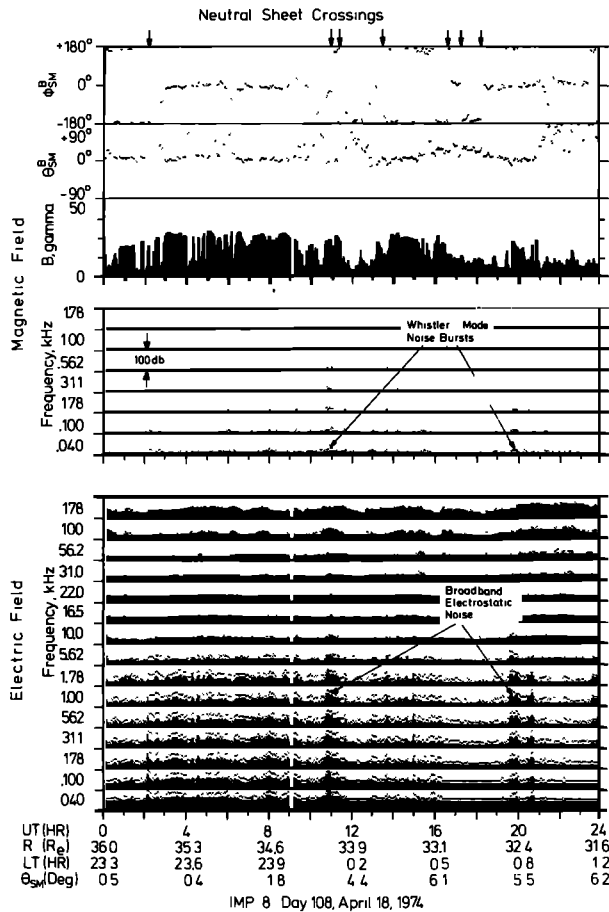


Fig. 5. Magnetic field and plasma wave measurements made by the Imp 8 spacecraft for day 108 during a transit of the neutral sheet [Gurnett *et al.*, 1976]. Note the intense electrostatic and magnetic noise bursts which occurred throughout the day.

electrons can participate in the resonance. On the other hand, when  $\beta \approx 1$  and  $T_e \approx T_i$ , we find that  $V_r^2 \approx v_e^2$ , which permits a substantial number of electrons to be involved in the resonance. In fact, in this regime the electron-wave resonance can stabilize the instability [Davidson *et al.*, 1977]. Thus in an initially unstable situation it is possible that the ensuing turbulence may sufficiently broaden the electron-wave resonance to stabilize the instability [Dupree, 1967; Weinstock, 1969]. However, numerical techniques are required to determine the saturation energy in the interesting regime  $\beta \approx 1$  and  $T_e \approx T_i$ . We note that this saturation mechanism can produce steady state turbulence, in contrast to the other stabilization processes discussed which only produce transient effects [Papadopoulos, 1977].

It is reasonable to expect  $T_e \lesssim T_i$ ,  $V_{at} \lesssim 3v_i$ , and  $\beta \sim O(1)$  for average plasma conditions in the magnetotail. For this parameter regime we anticipate that the dominant saturation mechanisms will be either current relaxation or electron resonance broadening. We present Figure 4, which is a comparison of the saturation energies due to these stabilization processes as a function of  $T_e/T_i$  and  $V_{at}/v_i$ . We choose  $\beta = 1.0$  and  $\omega_{pe}^2/\Omega_e^2 = 100$ . Clearly, current relaxation and electron resonance broadening are competitive processes in the regime  $T_e \lesssim T_i$  and  $V_{at} \lesssim v_i$ . For inhomogeneities whose scale lengths are of the order of the mean ion Larmor radius or larger ( $|V_{at}| \lesssim v_i$ ) we estimate the saturation energy to be  $(\epsilon_F/nT_i)_{\text{sat}} \lesssim 10^{-5}$ . We comment that the resonance broadening results include finite  $\beta$

electromagnetic corrections, which is an extension of the work of Huba and Papadopoulos [1978].

### 3. OBSERVATIONAL RESULTS

In this section we briefly review the experimental evidence of electrostatic and magnetic noise observed by Gurnett *et al.* [1976] in the distant magnetotail. An excellent example of this turbulence is shown in Figure 5. These measurements were made by the Imp 8 spacecraft during a transit of the neutral sheet on April 18, 1974, and are typical of neutral sheet crossings.

The electrostatic noise occurs over a broad frequency range extending from about 10 Hz to a few kilohertz, as may be seen in Figure 5. The frequency spectrum of the average electric field fluctuations during a high-intensity burst (occurring during the time 1056–1059 UT on day 108) is shown in Figure 6. During this 3-min period the local electron gyrofrequency was approximately 300 Hz, indicating that the largest field fluctuations occur for frequencies below the electron cyclotron frequency. Although instrumental limitations prevent measurement of very low frequencies, the spectral curve appears to be approaching a maximum in the vicinity of  $f \approx 10$  Hz. Frequency-time spectrograms indicate that the most intense noise is typically in the frequency range 10–70 Hz (see Figure 7), indicating that the detailed 3-min spectrum in Figure 6 is not unusual. The frequency spectrum of the peak electrostatic fluctuations has the same shape as that of the average electrostatic fluctuations but with an amplitude 3–5 times the corresponding average fluctuation amplitude. The amplitude of the peak electrostatic fluctuations is in the range  $|\delta E| = 0.05$ –5 mV/m. Finally, we mention that the orientation of the turbulent electric fields is observed to be within  $\pm 20^\circ$  from the perpendicular to the ambient magnetic field.

The magnetic noise is observed in the frequency range  $f \approx 10$ –600 Hz and is strongly correlated with the electrostatic noise (as seen in Figure 5) but occurs less frequently. The frequency spectrum of the magnetic fluctuations during the aforementioned intense electrostatic burst is shown in Figure 8. This spectrum is similar to the electric field spectrum, al-

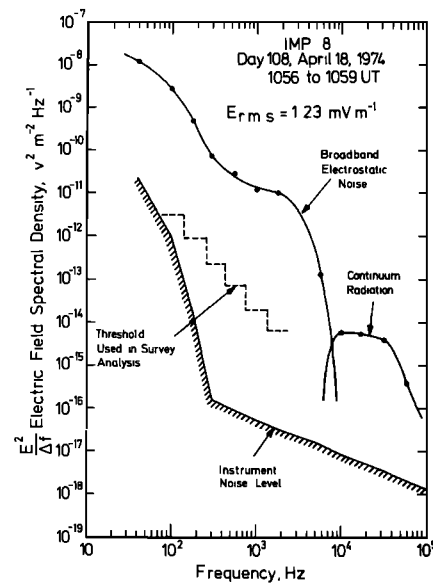


Fig. 6. A typical spectrum of broadband electrostatic noise during a period of relatively high intensity, from 1056 to 1059 UT on day 108 [Gurnett *et al.*, 1976].

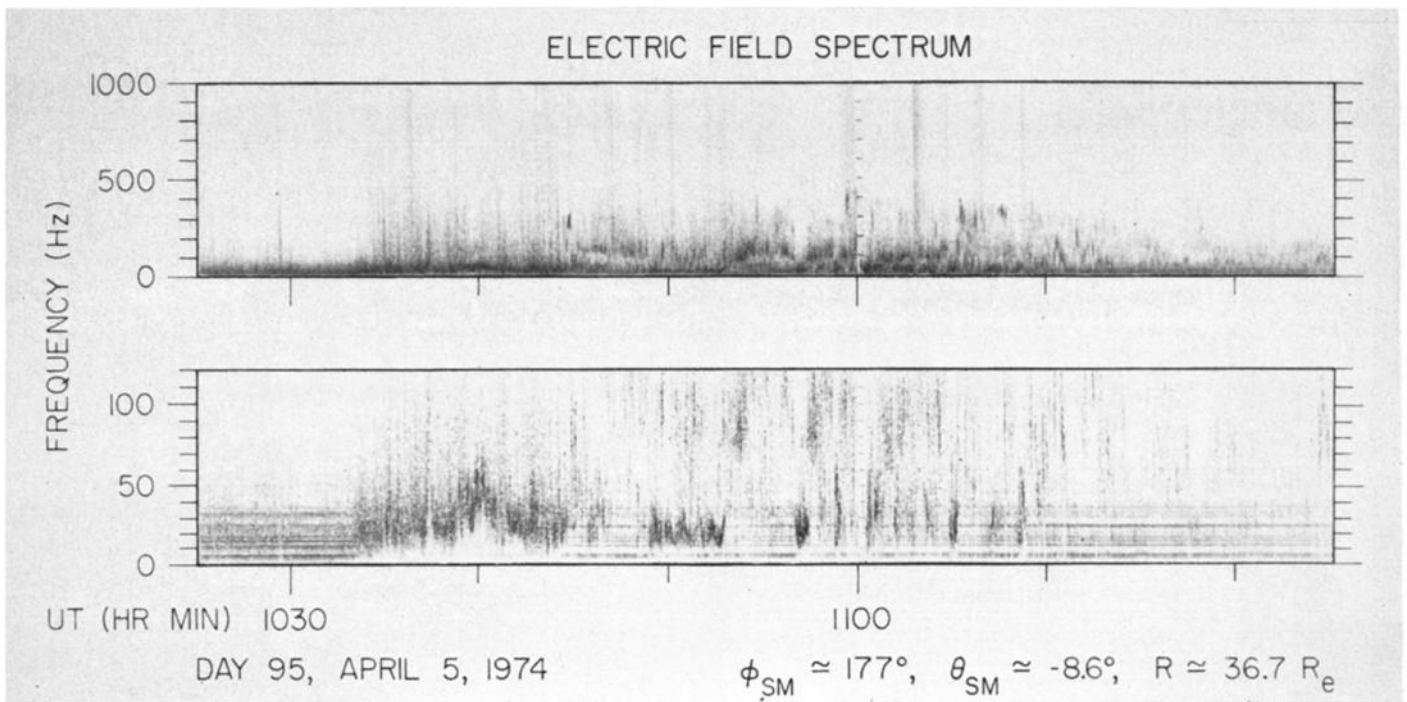


Fig. 7. Frequency-time spectrogram of the broadband electrostatic noise. Note that the most intense noise is in the range 10–70 Hz [Gurnett *et al.*, 1976].

though the magnetic noise seems to be more bursty (since its peak to average ratio is large), a finding which is consistent with its less frequent observation. The amplitude of this peak magnetic noise is in the range  $|\delta B| = 1\text{--}100$  m $\gamma$ . Unfortunately, the polarization of the magnetic field fluctuations could not be determined experimentally.

This microscopic turbulence is generally observed when the ambient magnetic field and plasma are turbulent and when

there are strong plasma flows ( $V_F \approx 500\text{--}2000$  km/s) toward or away from the earth [Frank *et al.*, 1976]. A typical turbulent state is illustrated in Figure 9, which plots the magnitude of the ambient magnetic field, proton density, proton temperature, and proton bulk velocity for 1030–1100 UT on day 108. The magnetic field is measured on a 1.28-s average, and the plasma data are measured on an 82-s average. The flow velocity and the proton temperature have not been plotted for 1046–1056, since the proton density is very low and the Lepedea measurements are not entirely reliable. We mention that a detailed analysis of a ‘fireball’ event by Coroniti *et al.* [1977] demonstrated that the magnetic field can be turbulent on time scales of  $\lesssim 1$  s, indicating the possibility of sharp gradients ( $L \approx r_{Li}$ ), which will be considered in the next section.

It is clear that even in as short a period as 30 min the satellite moved through a variety of plasma conditions. The magnetic field ranged from a few gammas up to 35  $\gamma$ , the density from 0.01 to 1.6  $\text{cm}^{-3}$ , the proton temperature from 1 to 10 keV, and the flow velocity from 300 to 1600 km/s. On the basis of these data we find that  $\beta$ , an important parameter in determining the existence and behavior of the lower-hybrid-drift instability, varies from  $10^2$  to  $10^{-2}$  over this period. This point is further discussed in the following section.

#### 4. COMPARISON OF THEORY AND OBSERVATIONAL RESULTS

In this section we compare the theoretical predictions of microturbulence associated with the lower-hybrid-drift instability discussed in section 2 with the recent satellite observations of electric and magnetic field fluctuations in the magnetotail [Gurnett *et al.*, 1976] detailed in section 3.

In particular, we demonstrate that the agreement of theory and experiment on such points as existence conditions for the instability, polarization of the turbulence, nature of the frequency spectrum of the fluctuations, and amplitude of the fluctuations is remarkably good. The detailed agreement of theory and experiment argues convincingly that the lower-hybrid-drift instability has been directly observed in the mag-

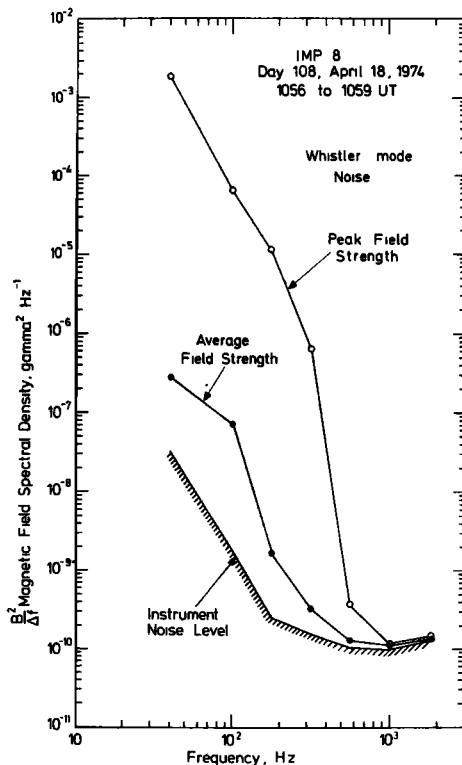


Fig. 8. Typical spectrum of magnetic noise from 1056 to 1059 UT on day 108 [Gurnett *et al.*, 1976].

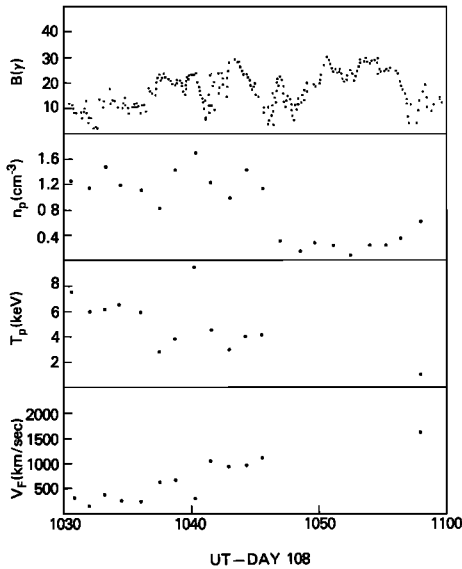


Fig. 9. Ambient magnetic field strength (R. P. Lepping, private communication, 1977), proton density, proton temperature, and proton bulk velocity (K. L. Ackerson, private communication, 1977) for 1030–1100 UT on day 108. Note that the magnetic field was very turbulent during this period. The data points for the bulk flow velocity and proton temperature are not shown for 1046–1056 UT, since the proton density is very low and the Lepedea measurements are not entirely reliable.

netotail. This is important, not only because this instability may be important in regulating magnetotail dynamics (e.g., reconnection and the triggering of magnetic substorms) but because it represents the first direct observation of an instability which is considered to be very important in several high  $\beta$  laboratory plasma devices (e.g., theta pinches and reversed field pinches).

The most striking feature of the satellite observations of Gurnett *et al.* [1976] is the strong correlation between the occurrence of electrostatic and electromagnetic noise and the presence of fluctuating magnetic fields (see Figure 5 and the discussion in section 3). The fluctuating magnetic fields imply the presence of magnetic field gradients and, furthermore, in situations in which the plasma beta is of order unity, gradients in the plasma density and temperature. Even in situations in which the magnetic field is relatively strong and constant there may exist density and temperature gradients if  $\beta \ll 1$ . In the theory of the lower-hybrid-drift instability discussed in section 2 we saw that plasma gradients with scale length satisfying  $L_n/r_{Li} < (m_i/m_e)^{1/4}$  were required to excite the lower-hybrid-drift instability. For typical tail parameters ( $T_i \sim 2$  keV and  $B \sim 15$   $\gamma$ ) it is found that  $r_{Li} \sim 300$  km, so that the instability can be excited for  $L_n \lesssim 2.0 \times 10^8$  km. However, as was noted earlier, for gradient scale lengths such that  $(m_i/m_e)^{1/2} < L_n/r_{Li} < (m_i/m_e)^{1/4}$  the mode transforms into the drift cyclotron instability [Friedberg and Gerwin, 1977; Gladd and Huba, 1978], which has a characteristic frequency and growth rate  $\omega_r \sim \Omega_i$  and  $\gamma \sim l(m_e/m_i)^{1/4}\Omega$ , respectively. Thus instability can persist even for  $L_n \sim 1.2 \times 10^4$  km.

Although the existence of gradients is obvious in Figure 9, it is somewhat difficult to ascertain their magnitude because the satellite offers only one reference point from which to observe magnetic field and plasma quantities, which can vary in both space and time. Indeed, the observations of plasma flow by the satellite show flow velocities that range up to 1600 km/s and are much larger than the average satellite velocity in the dis-

tant magnetotail ( $\approx 2$  km/s). We can estimate the gradient length scale from  $L = |\mathbf{V}_F + \mathbf{V}_s| \Delta t \approx V_F \Delta t$ , where  $\Delta t$  is the time over which the magnetic field or density changes appreciably,  $\mathbf{V}_F$  is the flow velocity of the plasma, and  $\mathbf{V}_s$  is the velocity of the satellite. If we consider Figure 9, we find that the gradient length scale in a turbulent region is  $L \approx 60,000$  km, where  $V_F \approx 1000$  km/s and  $\Delta t \approx 60$  s. Since we have assumed that the ion Larmor radius is  $r_{Li} \approx 50$ –400 km, we find that  $L/r_{Li} \approx 150$ –1200, which is too weak to excite the lower-hybrid-drift instability. However, the profiles in Figure 9 do not rule out the presence of sharper gradients, as mentioned in section 3. The microscopic structure of the magnetic field in a turbulent part of the magnetotail has been studied in detail by Coroniti *et al.* [1977]. In particular, Figure 3 of Coroniti *et al.* indicates that magnetic field gradient scale lengths can be as strong as  $L \sim r_{Li}$ . Unfortunately, measurements of density and temperature can only be made on an 82-s average, and the direct observation of sharp plasma gradients is not possible. However, if we consider the plasma to be in equilibrium locally, then we expect  $L_n \propto L_B \beta$ , where  $L_B$  is the scale length of the magnetic field inhomogeneity, and we can infer the existence of sharp plasma density gradients. Therefore we see that in the turbulent plasma sheet there can be ample plasma and field gradients of sufficient sharpness to excite the lower-hybrid-drift instability.

Having shown that the existence conditions for the lower-hybrid-drift instability can be met in the magnetotail, we now use the theory of section 2 to account for features of the electrostatic and electromagnetic noise. First we consider the polarization of the electrostatic noise. In developing the electrostatic theory it was found that the most rapidly growing part of the lower-hybrid-drift spectrum typically satisfies  $\mathbf{k} \times \delta \mathbf{E} \approx 0$  and  $\delta \mathbf{E} \cdot \mathbf{B}_0 \approx 0$ . In the work of Gurnett *et al.* [1976] it is shown that during a 30-min period in which the direction of the magnetic field was well established, the polarization of the electrostatic noise was always within  $\pm 20^\circ$  of perpendicular to the magnetic field and was thus consistent with the theoretical prediction that the most rapidly growing modes would be flutelike ( $\mathbf{k} \cdot \mathbf{B} \approx 0$ ). Although the lower-hybrid-drift instability is damped at large angles, propagation effects in an inhomogeneous medium may account for the observed angular distribution of the fluctuating electric field.

We next address the question of the relationship of the electrostatic and the electromagnetic noise. In the theory of the lower-hybrid-drift instability it is found that in a finite  $\beta$  plasma the important field components are  $\delta E_y$  and  $\delta B_z$  with

$$|\delta B_z|/|\delta E_y| \approx \beta_i^{1/2} (\omega_{pe}/\Omega_e) 10^8 \text{ m}\gamma \quad (21)$$

where  $\delta E_y$  is measured in millivolts per meter. Equation (21) is obtained in the approximation  $L_n/r_{Li} > 1$  and  $T_e/T_i \ll 1$ . Therefore when the plasma  $\beta_i$  is finite, the satellite should observe fluctuations in both  $\delta E_y$  and  $\delta B_z$ . The fact that the electrostatic noise is observed more frequently than the electromagnetic noise may be due to the relative sensitivity of the measuring devices (i.e., the magnetic field detectors are not as sensitive as the electric field detectors). We note that in (21) the relationship  $|\delta B_z|/|\delta E_y|$  is independent of the driving mechanism (i.e.,  $L_n/r_{Li}$ ) and we should see large  $|\delta B_z|$  whenever we see large  $|\delta E_y|$ . This is borne out by the experimental observations (Figure 5), in which we see that observation of electromagnetic noise is almost always attendant to the occurrence of exceptionally strong bursts of electrostatic noise.

As another example of finite  $\beta$  effects on the lower-hybrid-drift instability, we note that if  $T_e \lesssim T_i$ , finite  $\beta$  is a strong

stabilizing effect on the instability (see Figure 3). Close examination of the electrostatic turbulence that occurs during the 30-min time period illustrated in Figure 9 shows that the noise level in the last half of that time period is as much as 4 orders of magnitude larger than the noise in the first half. Examination of the profiles in Figure 9 indicates that the average plasma  $\beta$  during the latter half of the period is much lower than the average plasma  $\beta$  during the first half. This strongly suggests that the instability was finite  $\beta$  stabilized (or at least substantially curtailed) in growth during the first half, as would be expected from the theory.

Next, we turn our attention to the question of whether the frequency spectrum of the electrostatic noise is consistent with the theoretical predictions of the lower-hybrid-drift instability. First, consider the spectrum illustrated in Figure 2. We note that the  $k$  spectrum is quite broad ( $\gamma$  is substantial for  $0.5 < kr_{Le} < 5$ ), while the real frequency in this range varies only by a factor of 2. Therefore we might expect to see a relatively narrow frequency spectrum centered about  $\omega_{lh}$ . The actual center frequency will depend on the sharpness of the gradient exciting the mode. However, the frequency observed by the satellite includes the relevant Doppler shifts, since in general, proton bulk flows are not directed parallel to the local magnetic field vector [Frank *et al.*, 1976]. Thus

$$f_{\text{obs}} = f + [(\mathbf{k} \cdot \mathbf{V}_s)/2\pi] + [(\mathbf{k} \cdot \mathbf{V}_F)/2\pi] \quad (22)$$

Typically,  $V_F \gg V_s$ , so that

$$f_{\text{obs}} \sim f \pm (kV_F/2\pi) \cos \phi \quad (23)$$

For typical tail parameters we estimate the range of wave numbers excited to be  $k \approx 0.2\text{--}5 \text{ km}^{-1}$ , maximum growth occurring at  $k_M \approx 1 \text{ km}^{-1}$ . Moreover, if we let  $V_F = 500\text{--}1500 \text{ km/s}$ ,  $f \sim f_{lh} \sim 3\text{--}20 \text{ Hz}$ , and  $\cos \phi \sim \frac{1}{2}$ , it is found that  $f_{\text{obs}} \approx 10\text{--}600 \text{ Hz}$  with the maximum intensity ( $f_{\text{obs}}^M$ ) in the range  $f_{\text{obs}}^M \approx 20\text{--}60 \text{ Hz}$ , which is consistent with the observations of Gurnett *et al.* [1976] (see Figure 7). Thus while the theory of section 2 predicts a relatively narrow frequency spectrum, the dominance of the Doppler-shifting term  $\mathbf{k} \cdot \mathbf{V}_F$  in (23) acts to broaden the observed spectrum substantially.

Furthermore, the Doppler shift explains the energy frequency spectra (Figures 6 and 8) discussed in the previous section. In these figures the amplitude of fluctuations decreases with increasing frequency. From nonlinear considerations we find that as  $k$  increases above  $k_M$ , the saturation energy of the excited waves decreases. Moreover, since these waves are strongly Doppler-shifted to higher frequencies, we expect the energy density of the unstable waves to be a decreasing function of frequency for  $\omega > \omega_M$ , which is consistent with Figures 6 and 8.

Finally, we consider whether the theoretical amplitudes of the electrostatic and electromagnetic noise are consistent with observations. In section 2, several saturation mechanisms which could stabilize the lower-hybrid-drift instability were discussed. It is not clear which of these mechanisms is dominant or, as might reasonably be expected, whether there are mechanisms which might be important under some plasma conditions and not under others. For purposes of comparison with observation we determine the strengths of the fluctuating fields, using the estimate of the saturation energy based upon current relaxation. The amplitude of the electric field fluctuations is

$$|\delta E| = (\pi n m_e V_{dt}^2)^{1/2} (1 + T_e/T_i)(1 + \omega_{pe}^2/\Omega_e^2)^{-1/2}$$

and the amplitude of the magnetic fluctuations is

$$|\delta B| = \frac{v_i}{c} \left( \frac{m_i}{m_e} \right)^{1/2} \frac{\omega_{pe}^2}{\Omega_e^2} |\delta E| 10^8 \text{ m}\gamma$$

For conditions typical of the magnetotail (e.g.,  $T_i = 1 \text{ keV}$ ,  $B = 20 \gamma$ ,  $n \sim 0.01\text{--}1 \text{ cm}^{-3}$ ,  $T_e \ll T_i$ , and  $V_{dt} \lesssim v_i$ ) we find from (19) and (20) that  $|\delta E| \sim 0.2\text{--}6 \text{ mV/m}$  and  $|\delta B| \sim 0.09\text{--}270 \text{ m}\gamma$ , which is consistent with experimental evidence, in which the amplitude of the peak electric field fluctuations is observed to be in the range of  $|\delta E| \sim 0.05\text{--}5 \text{ mV/m}$  and that of the magnetic field fluctuations is  $|\delta B| \sim 1\text{--}100 \text{ m}\gamma$ .

## 5. CONCLUSIONS AND DISCUSSION

We have demonstrated that our theoretical prediction of plasma turbulence in the magnetotail due to the lower-hybrid-drift instability [Huba *et al.*, 1977] is substantiated by experimental observations of electrostatic and magnetic turbulence in the distant magnetotail [Gurnett *et al.*, 1976]. In particular, we have shown that existence conditions for the lower-hybrid-drift instability can be met (i.e., there seem to exist sharp localized gradients within a much broader plasma sheet). Second, we have shown that observations of the frequency spectrum and polarization are in good agreement with the predictions of our linear stability analysis. Third, we have shown that the observed amplitude of fluctuations is consistent with the nonlinear analysis of the lower-hybrid-drift mode. Finally, we point out that both the electrostatic and the magnetic fluctuations observed by Gurnett *et al.* [1976] may be explained by this single instability. In addition to discussing the specific points above, we have presented a short review of the theory of the lower-hybrid-drift instability because of its relative newness to the space physics community. We now address several other topics pertinent to the problem of microturbulence in the magnetotail.

The theory of the lower-hybrid-drift instability discussed in this work has emphasized the physical nature of the instability and retained only the fundamental aspects of the plasma configuration (e.g., magnetic field and density inhomogeneities and finite  $\beta$ ). However, in the turbulent plasma sheet, other aspects of the plasma environment which affect the lower-hybrid-drift instability, such as temperature gradients [Davidson *et al.*, 1977; Krall and McBride, 1976], magnetic shear [Krall, 1977; Gladd *et al.*, 1977; Davidson *et al.*, 1978], and magnetic curvature [Krall and McBride, 1976] can be important at times. The inclusion of all these effects is beyond the scope of this paper. We point out that although the instability theory presented here is incomplete, the instability is viable for a variety of plasma conditions typical of the magnetotail.

The most important aspect of the observed turbulence is that it strongly suggests that anomalous transport is indeed a major factor in the evolution of macroscopic processes such as field line merging, tearing instabilities, or fireballs [Frank *et al.*, 1976; Coroniti *et al.*, 1977]. Probably the only tractable method for realistically describing such macroscopic events is through the use of multifluid plasma codes which incorporate anomalous transport coefficients based upon the relevant microscopic physical phenomena. The evidence presented in this paper indicates that we may proceed with some confidence to use the anomalous transport properties associated with the lower-hybrid-drift instability in a multifluid code to model macroprocesses in the magnetotail. We are presently developing such a code for the purposes of understanding reconnection in the magnetotail.

We comment that a problem encountered in invoking the lower-hybrid-drift instability as a source of anomalous resistivity for magnetic field line reconnection is the absence of instability near magnetic nulls. This is because as  $B \rightarrow 0$ , one expects  $\beta \rightarrow \infty$ , and the instability is easily stabilized [e.g., Huba et al., 1977, Figure 2]. Moreover, near a magnetic null the electron orbits become complex [Hoh, 1966] and are no longer describable by the guiding center drift approximation used in the theory. However, a model of the magnetotail with a well-defined neutral line embedded in the plasma sheet is a considerable oversimplification of the physical situation. In fact, the plasma sheet is a very turbulent medium, as is shown by Gurnett et al. [1976], Frank et al. [1976], and Coroniti et al. [1977]. Thus we suggest that the lower-hybrid-drift instability (and possibly other instabilities) produces small-scale 'clumps' of electrostatic turbulence throughout the magnetotail and that electrons can be effectively scattered by these clumps. A macroscopic anomalous resistivity based on a statistical description of these clumps can then exist in the magnetotail, and the absence of turbulence at a single magnetic null point is of little consequence.

Within the context of this concept of anomalous resistivity produced by small-scale clumps of lower-hybrid-drift turbulence we suggest that a mode-mode coupling process may occur in the magnetotail, similar to that which occurs in the ionosphere. Ionospheric irregularities have been observed with scale lengths from a few meters to a few kilometers [Dyson et al., 1974]. Since no single instability has been found which can explain the entire range of irregularities, the prevailing theories [Sudan et al., 1973; Chaturvedi and Kaw, 1976] invoke a two-step process. A long-wavelength instability (e.g., Rayleigh-Taylor instability) is excited which can nonlinearly produce short-wavelength drift waves. We propose that a similar phenomenon may exist in the magnetotail, whereby a macroscopic MHD instability (e.g., a kink or tearing mode) can produce local gradients in density and magnetic field which can excite short-wavelength modes such as the lower-hybrid-drift instability. The anomalous resistivity produced by the ensuing clumps of electrostatic turbulence will in turn affect the evolution of the large-scale disturbance. We are presently investigating this possibility and hope eventually to perform a numerical simulation which will self-consistently follow this process.

Finally, we reiterate that the lower-hybrid-drift instability is an important anomalous transport mechanism in many laboratory plasma confinement devices, such as theta pinches, reversed field pinches, and mirror machines. Coincidentally, many of the important dimensionless quantities which determine the behavior of this instability are the same for both the laboratory and the magnetotail plasma (e.g.,  $\omega_{pe}^2 \gg \Omega_e^2$ ,  $\beta \sim 1$ , and  $V_{di} \sim v_i$ ), even though the density and magnetic field differ by many orders of magnitude. Unfortunately, the lower-hybrid-drift instability cannot be observed directly in laboratory experiments, since its time scale is extremely short ( $t_{ih} = f_{ih}^{-1} \sim 10^{-9}$  s). Thus the magnetotail may be the ideal laboratory to study the lower-hybrid-drift instability because in situ measurements can be made. The information obtained from such studies may prove to be very valuable to the ongoing research in plasma confinement experiments and fusion research.

*Acknowledgments.* We gratefully acknowledge Don Gurnett for calling our attention to the observational measurements and for several valuable discussions. We also wish to thank Don Gurnett and Kent Ackerson for providing field fluctuation and particle data, respectively, and Ron Lepping for providing magnetometer data. Fi-

nally, we thank Geary Voots and Mark Baumbach for their assistance in preparing the fluctuation data. This research has been supported by the Office of Naval Research and NASA.

The Editor thanks F. V. Coroniti for his assistance in evaluating this paper.

#### REFERENCES

- Ashour-Abdalla, M., and C. F. Kennel, Convective cold upper hybrid instabilities, in *Magnetospheric Particles and Fields*, edited by B. M. McCormac, D. Reidel, Hingham, Mass., 1976.
- Chaturvedi, P. K., and P. Kaw, An interpretation for the power spectrum of spread  $F$  irregularities, *J. Geophys. Res.*, **81**, 3257, 1976.
- Comisso, R. J., and H. R. Griem, Observation of collisionless heating and thermalization of ions in a theta pinch, *Phys. Rev. Lett.*, **36**, 1038, 1976.
- Coroniti, F. V., F. L. Scarf, L. A. Frank, and R. P. Lepping, Microstructure of a magnetotail fireball, *Geophys. Res. Lett.*, **4**, 219, 1977.
- Davidson, R. C., Quasilinear stabilization of the lower-hybrid-drift instability in post-implosion theta pinches, submitted to *Phys. Fluids*, 1977.
- Davidson, R. C., and N. T. Gladd, Anomalous transport properties of the lower-hybrid-drift instability, *Phys. Fluids*, **18**, 1327, 1975.
- Davidson, R. C., and N. T. Gladd, Influence of strong inhomogeneities in high-frequency mirror-drift-cone and convective-loss-cone instabilities, *Phys. Fluids*, **20**, 1516, 1977.
- Davidson, R. C., N. T. Gladd, C. S. Wu, and J. D. Huba, Influence of finite- $\beta$  effects on the lower-hybrid-drift instability in post-implosion  $\theta$  pinches, *Phys. Rev. Lett.*, **37**, 750, 1976.
- Davidson, R. C., N. T. Gladd, C. S. Wu, and J. D. Huba, Effects of finite plasma beta on the lower-hybrid-drift instability, *Phys. Fluids*, **20**, 301, 1977.
- Davidson, R. C., N. T. Gladd, and Y. Goren, Influence of magnetic shear on the lower-hybrid-drift instability in toroidal reversed-field pinches, *Phys. Fluids*, **21**, 992, 1978.
- Dupree, T. H., Nonlinear theory of drift-wave turbulence and enhanced diffusion, *Phys. Fluids*, **10**, 1049, 1967.
- Dyson, P. L., J. P. McClure, and W. B. Hanson, In situ measurements of the spectral characteristics of ionospheric irregularities, *J. Geophys. Res.*, **79**, 1497, 1974.
- Frank, L. A., K. L. Ackerson, and R. P. Lepping, On hot tenuous plasmas, fireballs, and boundary layers in the earth's magnetotail, *J. Geophys. Res.*, **81**, 5859, 1976.
- Fredericks, R. W., Plasma instability at  $(n + \frac{1}{2})f_c$  and its relationship to some satellite observations, *J. Geophys. Res.*, **76**, 5344, 1971.
- Friedberg, J. P., and R. A. Gerwin, Lower-hybrid-drift instability at low drift velocities, *Phys. Fluids*, **20**, 1311, 1977.
- Gladd, N. T., The lower-hybrid-drift instability and the modified two-stream instability in high density theta pinch environments, *Plasma Phys.*, **18**, 27, 1976.
- Gladd, N. T., and J. D. Huba, Finite beta effects on the drift cyclotron instability, submitted to *Phys. Fluids*, 1978.
- Gladd, N. T., Y. Goren, C. S. Lui, and R. C. Davidson, Influence of strong inhomogeneities and magnetic shear on microstability properties of the torus sheath, *Phys. Fluids*, **20**, 1876, 1977.
- Gurnett, D. A., L. A. Frank, and R. P. Lepping, Plasma waves in the distant magnetotail, *J. Geophys. Res.*, **81**, 6059, 1976.
- Hoh, F. C., Stability of sheet pinch, *Phys. Fluids*, **9**, 277, 1966.
- Huba, J. D., and K. Papadopoulos, Nonlinear stabilization of the lower-hybrid-drift instability by electron resonance broadening, *Phys. Fluids*, **21**, 121, 1978.
- Huba, J. D., and C. S. Wu, Effects of a magnetic field gradient on the lower-hybrid-drift instability, *Phys. Fluids*, **19**, 988, 1976.
- Huba, J. D., N. T. Gladd, and K. Papadopoulos, The lower-hybrid-drift instability as a source of anomalous resistivity for magnetic field line reconnection, *Geophys. Res. Lett.*, **4**, 125, 1977.
- Krall, N. A., Drift waves, in *Advances in Plasma Physics*, vol. 1, edited by A. Simon and W. B. Thompson, p. 153, John Wiley, New York, 1968.
- Krall, N. A., Shear stabilization of lower hybrid drift instabilities, *Phys. Fluids*, **20**, 311, 1977.
- Krall, N. A., and P. C. Liewer, Low frequency instabilities in magnetic pulses, *Phys. Rev. A*, **4**, 2094, 1971.
- Krall, N. A., and J. B. McBride, Magnetic curvature and ion distribution function effects on lower-hybrid-drift instabilities, *Phys. Fluids*, **19**, 1970, 1976.
- Mikhailovskii, A. B., and A. V. Timofeev, Theory of cyclotron instability in a non-uniform plasma, *Sov. Phys. JETP*, **17**, 626, 1963.

- Papadopoulos, K., A review of anomalous resistivity for the ionosphere, *Rev. Geophys. Space Phys.*, *15*, 113, 1977.
- Sudan, R. N., J. Akinrimisi, and D. T. Farley, Generation of small-scale irregularities in the equatorial electrojet, *J. Geophys. Res.*, *78*, 240, 1973.
- Weinstock, J., Formulation of a statistical theory of strong plasma turbulence, *Phys. Fluids*, *12*, 1045, 1969.
- Winske, D., and P. C. Liewer, Particle simulation studies of the lower-hybrid-drift instability, submitted to *Phys. Fluids*, *21*, 1017, 1978.
- Young, P. S., J. D. Callen, and J. E. McCune, High-frequency electrostatic waves in the magnetosphere, *J. Geophys. Res.*, *78*, 1082, 1973.

(Received March 16, 1978;  
revised June 5, 1978;  
accepted June 28, 1978.)